Research Square

Preprints are preliminary reports that have not undergone peer review.
They should not be considered conclusive, used to inform clinical practice,
or referenced by the media as validated information.

Human Umbilical Cord–Derived Mesenchymal Stromal Cell Therapy Modulates Inflammation in Mine-Explosive Wounds in Humans: A Transcriptomic Study

Volodymyr Shablii

shabliy@stemcellclinic.com.ua

Institute of Cell Therapy

Elvina Valatkaitė

Institute of Biochemistry, Life Sciences Center, Vilnius University

Yevhen Symulyk

O. O. Shalimov National Scientific Center of Surgery and Transplantology of the National Academy of Medical Sciences of Ukraineuk

Tetiana Bukreieva

Institute of Cell Therapy

Alina Ustymenko

M. D. Strazhesko National Scientific Center of Cardiology, Clinical and Regenerative Medicine of the National Academy of Medical Sciences of Ukraine

Ihor Zahanich

Institute of Cell Therapy

Vitalii Kyryk

M. D. Strazhesko National Scientific Center of Cardiology, Clinical and Regenerative Medicine of the National Academy of Medical Sciences of Ukraine

Inessa Skrypkina

Institute of Molecular Biology and Genetics of the National Academy of Science of Ukraine

Ruslan Saliutin

O. O. Shalimov National Scientific Center of Surgery and Transplantology of the National Academy of Medical Sciences of Ukraineuk

Giedrė Valiulienė

Institute of Biochemistry, Life Sciences Center, Vilnius University

Deimantė Šulijienė

Institute of Biochemistry, Life Sciences Center, Vilnius University

Aistė Zentelytė

Institute of Biochemistry, Life Sciences Center, Vilnius University

Veronika Borutinskaitė
Institute of Biochemistry, Life Sciences Center, Vilnius University
Rūta Navakauskienė
Institute of Biochemistry, Life Sciences Center, Vilnius University

Research Article

Keywords: human umbilical cord–derived mesenchymal stromal cells, MSC, mine-explosive injury, transcriptome profiling, wound, soft tissue injury, MSC-based therapy, cell therapy

Posted Date: April 3rd, 2026

DOI: https://doi.org/10.21203/rs.3.rs-8701993/v1

License: This work is licensed under a Creative Commons Attribution 4.0 International License.
Read Full License

Additional Declarations: No competing interests reported.

Abstract

Background

The effective treatment of blast-related soft tissue injuries requires the development of innovative approaches. MSCs have demonstrated paracrine beneficial effects by regulating inflammation, modulating fibroblast activation and collagen production, and promoting neovascularization and re-epithelialization. This research focused on how wound functional status and transcriptome changed following umbilical cord-derived mesenchymal stromal cell transplantation in patients with mine explosive wounds of the lower limbs.

Methods

This study involved 7 patients following conventional wound treatment (control group) and 8 patients treated with a single dose of intra-wound injection of human umbilical cord-derived mesenchymal stromal cells (hUC-MSCs) (MCS group). RNA-seq of wound biopsy specimens was used for transcriptome analysis, and selected mRNA expression levels were validated by real-time quantitative PCR (qPCR). Data was collected on the day of patient admission (day 0) and on the 1^{st} and 7^{th} days of follow-up. Surgical autoplasty was applied as a treatment method for wound closure. To assess potency, hUC-MSCs were co-cultured with various immune cells, followed by flow cytometry and qPCR analyses.

Results

In the present study, we demonstrated that hUC-MSCs transplantation was safe and did not affect the wound healing rate or the efficiency of surgical autoplasty in patients with mine-explosive wounds within one week. hUC-MSCs injections exerted anti-inflammatory effects in wounds at the transcriptomic level. Gene expression changes observed in macrophages and $CD4^+$ T cells in MSC co-culture models further support the immunomodulatory potency of hUC-MSCs in attenuating inflammation in mine-explosive wounds.

Conclusions

hUC-MSCs transplantation was shown to be safe and did not adversely affect wound healing or surgical autoplasty outcomes, while demonstrating pronounced anti-inflammatory effects within one week of observation.

Trial registration

This study was conducted as a prospective, single-center, open-label, non-randomized clinical study. All procedures were performed in accordance with the Declaration of Helsinki and were approved by the local Ethics Committee of O.O. Shalimov National Scientific Center of Surgery and Transplantology (protocol #10/05/2024).

Introduction

Large traumatic soft tissue wounds, in particular mine-blast injuries, require new effective treatment approaches. All military operations are the cause of suffering for both military personnel and civilians with mine-explosive wounds that require adequate treatment. By July 2025, the number of civilians injured by explosive weapon use in Ukraine since the Russian invasion began on 24 Feb 2022 had reached 29,748 [1]. The number of casualties among military personnel, both killed and wounded, is a state secret in Ukraine due to the ongoing war; however, Western analysts estimate the number to be ten times higher than civilians [2, 3]. Blast-related injuries are frequently associated with extensive soft tissue destruction, contamination, ischemia, and complex combined trauma. These factors significantly complicate timely wound closure and increase the risk of long-term complications, including chronic infection and functional impairment. Conventional surgical management is often limited by inadequate wound granulation and excessive scar formation, particularly in large or complex defects. Consequently, regenerative strategies are increasingly being explored as adjunctive treatments to standard surgery.

Mesenchymal stromal cells (MSCs) are known for their immunomodulatory properties and have been applied in the treatment of various conditions, including osteoarthritis, rheumatoid arthritis, and acute respiratory distress syndrome [4–7]. MSCs or their derived products have demonstrated beneficial paracrine effects by modulating inflammation, regulating fibroblast activation and collagen production, and promoting neovascularization and re-epithelialization [8, 9]. However, data on the impact of MSCs on wound healing and their immunomodulatory properties in humans, particularly in the context of acute traumatic wounds, remain limited. A meta-analysis demonstrated that MSC-based therapy can accelerate the healing of diabetic ulcers, reduce pain, preserve limbs, and improve prognosis compared with conventional treatment [10]. These findings suggest that local administration of human umbilical cord-derived MSCs (hUC-MSCs) may enhance the healing of landmine-explosive wounds of the extremities.

However, the mechanisms through which MSCs influence wound healing are not yet fully understood. Most studies have been conducted on experimental models, and findings from laboratory animals do not fully reflect the complex pathogenesis of mine-explosive wounds in humans. The standard surgical treatment strategy for patients with mine-explosive injuries includes careful preparation of the recipient wound bed, ensuring successful engraftment of both free flaps and non-vascularized skin grafts [11, 12]. The severe inflammation and extensive soft tissue trauma characteristic of mine-explosive wounds result in delayed granulation and vasculogenesis, which should be addressed to improve autograft engraftment [13, 14]. Furthermore, the compensatory effort of mine-explosive wounds to closure and epithelialization can accelerate scar formation.

Therefore, the transplantation of hUC-MSCs could represent a promising therapeutic approach to reduce wound inflammation, stimulate granulation tissue formation and enhance vascularization of the wound bed, thereby creating optimal conditions for closure of large and complex lower extremity defects. Furthermore, the study of the molecular biological effects of MSC therapy in the regeneration of limb

mine-explosive wounds may provide insights into the underlying mechanisms of their therapeutic action in humans.

Materials and methods

Participants and study design

A prospective, single-center, open-label, non-randomized study was conducted at the O. O. Shalimov National Scientific Center of Surgery and Transplantology, Kyiv, Ukraine, from February 2024 to November 2024.

The methods employed in this study included general clinical assessments (physical examination), laboratory tests (complete blood count, biochemical blood tests, wound microflora analysis, and PCR), and instrumental procedures (angiography and wound biopsy).

A total of 15 patients (men aged 22 to 56 years) were initially enrolled in the study. Seven patients who received treatment with Betadine (CJSC Pharmaceutical Plant EGIS, Hungary) or Levomekol (PJSC Farmak, Ukraine) were assigned to the control group. The MSC group consisted of eight patients who, in addition to conventional therapy, received a local injection of a single dose of hUC-MSCs. The inclusion criteria were as follows: mine-explosive injuries of the upper/ lower limbs; the wound surface area does not exceed 600 cm^2; blood glucose < 7 mmol/L; HbA1c < 6.0%; number of microorganisms in the wound culture during the screening period < 10^7; adequate blood supply to the limb demonstrated by any instrumental method (Doppler ultrasonography of the lower extremity arteries, CT angiography, or laser Doppler flowmetry); no planned amputation of the limb within the next 3 months according to the investigator; the participant's willingness to refrain from tobacco/nicotine use during the study; age 18–60 years.

The exclusion criteria were as follows: gangrene of a limb; acute kidney or liver failure; diagnosis of concomitant tumour in any organs; occurrence of severe and/or unexpected adverse events during the study potentially related to the use of the biological drug; withdrawal of the patient from further participation in the study, age < 18 or > 60 years. All participants provided written informed consent before enrollment.

hUC-MSCs isolation and preparation

Umbilical cords (UCs) obtained after Caesarean section were collected from 23- to 36-year-old donors at 39–41 weeks of gestation in the Kyiv city maternity hospital #3. All donors (n = 19) provided written informed consent for the collection and the use of their UCs in the approved clinical study. The UC quality assessment, donor screening, MSCs isolation, and cryopreservation were performed according to a previously published method [15]. Briefly, UC tissue pieces were plated into cell culture-treated flasks (Sarstedt, Nümbrecht, Germany) and covered with MEM alpha modification (Sigma, Irvine, UK)

supplemented with 15% FBS (Sigma, Paraguay origin, Saint Louis, MO, USA), 1× RPMI amino acid solution (Sigma, Irvine, UK), and 1× streptomycin/penicillin (Sigma, Irvine, UK), referred to as completed culture medium. Explants were incubated at 37°C in 5% CO_2 for 14 days, with medium changes twice a week. hUC-MSCs at passage 3 were harvested and cryopreserved using a rate-controlled freezer at a final concentration of 5% dimethyl sulfoxide (Sigma-Aldrich, Saint Louis, MO, USA) in HBSS (Sigma, Irvine, UK). Aliquots from all samples were collected for quality control.

Administration of hUC-MSCs

The release criteria for the clinical use of hUC-MSCs included the absence of contamination with pathogenic microorganisms (bacteria, mycoplasma, and fungi), a normal karyotype, and characteristic identity and purity profiles. Cells were required to be positive (≥ 95%) for CD73, CD90, and CD105, and negative (≤ 2%) for CD45 and CD34, expression in accordance with the minimal criteria for multipotent mesenchymal stromal cells established by the International Society for Cellular Therapy (ISCT) [16].

For local injections, hUC-MSCs at passage 3 were thawed in a water bath at 37°C until the liquid phase appeared. Cells were centrifuged at 300 ×g for 5 min at RT, and resuspended in a vehicle solution composed of saline (Darnytsya, Kyiv, Ukraine) and 5% human serum albumin (Biopharma, Kyiv, Ukraine). The average cell viability was 87.8 ± 5.1% before injection. Cells were administered as a single dose on the treatment day. The administered cell dose was calculated as 2.5×10^6 cells per 5 cm^2 applied to the wound bed and 1×10^6 cells per 4 cm along the wound perimeter of the affected lower limb, delivered via a series of 0.1 ml injections. During administration and for 30 minutes thereafter, the patient's blood pressure, body temperature, pulse, and skin color were continuously monitored. No serious adverse events (SAEs) were observed during or after MSC administration.

Wound biopsy

Wound biopsies were collected before treatment on the day of inclusion (day 0), 24 hours, and 7 days after hUC-MSC administration. In the control group, biopsies were collected at the same time points. Wounds were treated with sterile saline and antiseptics along the edges. Biopsy samples (weighing 0.2–0.5 g) were excised to full thickness using a scalpel and placed in sterile cryotubes. Tubes were snap frozen in liquid nitrogen and stored at -80°C until further processing.

Assessment of wound surface area

Photographs of the wounds were taken before hUC-MSCs administration, immediately after, and at day 7. The wound surface area was assessed using ImageJ. The wound healing rate was calculated using the formula: Wound healing rate, % = $\frac{WA_0 - WA_7}{WA_0} \times 100\%$,

where: WA_0 – wound area at day 0, WA_7 – wound area at day 7.

Reconstructive surgical approaches for lower extremity defects

Closure of soft tissue defects of the lower extremities was performed based on the composition of the wound bed, the extent of tissue damage and the need for subsequent reconstructive interventions. In cases involving functional areas, such as joint osteosynthesis insertion or when future orthopedic interventions (e.g., osteosynthesis or plate insertion) were required, free microsurgical transplantation of skin-fat, skin-fascial, or skin-muscle flaps was performed. This approach ensured coverage of the defect with soft-elastic well-vascularized tissues. In other cases, when the wound bed consisted of muscle, the defect was not in a functional zone and no preparation for future surgical interventions was needed, autologous dermoplasty was performed using a non-vascularized, thinned full-thickness skin graft obtained with a dermatome. A non-vascularized skin graft allows for defect closure through diffusion from the adjacent recipient tissues, which requires high-quality granulations. Subsequently, after engraftment, these grafts form scar tissue in contrast to a freely transplanted vascularized tissue complex.

Isolation of PBMC, CD4+, CD14 + cells and their co-culture with hUC-MSCs

Human peripheral blood mononuclear cells (PBMC, n = 5) were isolated from peripheral blood samples of patients with mine-explosive wounds using density gradient centrifugation with Ficoll (Cytiva, Global Life Sciences Solutions, Marlborough, MA, USA). $CD4^+$ and $CD14^+$ cell subpopulations were purified from PBMCs using the MagniSort™ Human CD4 T cell 2-Step Enrichment Kit according to the manufacturer's instructions. PBMC, $CD4^+$, or $CD14^+$ cells were resuspended in RPMI-1640 media (Gibco, Life Technologies Corp., Carlsbad, CA, USA) supplemented with 10% heat-inactivated fetal bovine serum (FBS) and seeded in a 24-well plate at a total volume of 1000 µL. PBMCs and $CD4^+$ T cells were stimulated using Dynabeads® Human T-Activator CD3/CD28 (Life Technologies AS, Oslo, Norway) at a bead/cell ratio of 1:5 and 1:1, respectively. Differentiation of $CD14^+$ cells from PBMC into macrophages was performed in RPMI-1640 media, supplemented with 10% FBS and 50 ng/mL macrophage colony-stimulating factor (M-CSF) for 7 days, followed by polarization toward M1 phenotype using lipopolysaccharide (LPS, 100 ng/mL) and interferon-γ (IFN-γ, 20 ng/mL) for 24 hours.

hUC-MSCs from three donors were thawed and cultured as described above. The cells were incubated with mitomycin C (20 µg/mL) in complete culture medium for 2 hours, detached using 0.05% trypsin and 0.02% EDTA (Sigma, UK), washed, counted. hUC-MSCs from three donors were mixed in equal proportion (1:1:1) and then seeded into 0.4 µm ThinCerts™-TC insert (Greiner Bio-One, Monroe, NC, USA). Co-cultures of MSC: PBMC (1:5) and MSC: $CD4^+$ cells (1:10) were maintained at 37°C for 4 days and harvested for flow cytometry and RT-qPCR analyses.

Flow cytometry

The expression of surface markers on hUC-MSCs and PBMCs was analyzed by flow cytometry. For immunostaining, cells were incubated with fluorochrome-conjugated mouse anti-human monoclonal antibodies (all from BD Biosciences) targeting the following markers:

hUC-MSCs: CD34, CD45, CD73, CD90, CD105.

PBMCs: CD3, CD4, CD8, CD14, CD25, CD45, CD45RO, CD57, CD69, CD80, CD127, CD169, CD183, CD206, CD279.

Cells were stained according to the manufacturer's instructions, typically for 30 minutes at 4°C in the dark. After staining, cells were washed with BD CellWash buffer and then resuspended in 300 µL DPBS for acquisition. Data acquisition was performed using a BD FACSAria cell sorter (BD Biosciences). At least 20,000 events were collected per sample. Data were analyzed using BD FACSDiva 6.1.3 software (BD Biosciences), and results were expressed as the percentage of positive cells for each marker or cell population. Appropriate negative (unstained) and single-stained controls were included in each experiment to set voltages, establish gating, and perform fluorescence compensation.

RNA isolation, RNA-seq, and bioinformatics analysis

Samples were prepared in biological triplicate. RNA was extracted using a NucleoSpin RNA isolation kit (Macherey–Nagel, Hœrdt, France) according to the manufacturer's protocol. RNA-seq libraries were prepared using the Agilent SureSelect Automated Strand-Specific RNA Library Prep kit, with polyA selection by Novogene Co., Ltd. (Beijing, China). Prepared libraries were sequenced on an Illumina HiSeq2000, using a paired-end 150 bp sequencing strategy (short-reads) and 20M read pairs per sample. Raw data (in the fastq format) were first processed using the fastp software. In this step, clean data (clean reads) were obtained by removing reads containing adapters, reads containing poly-N, and low-quality reads from the raw data. At the same time, the Q20, Q30, and GC content of the clean data were calculated. All downstream analyses were based on high-quality, clean data. Raw paired-end sequence reads were mapped to the human transcriptome (ensembl_homo_sapiens_grch38_p12_gca_000001405_27) using Hisat2 v2.0.5. featureCounts v1.5.0-p3 was used to count the read numbers mapped to each gene. Then, the FPKM of each gene was calculated based on the gene's length and the read count mapped to that gene. Differential expression analysis was performed using the DESeq2 R package (1.20.0). Genes with adjusted p-value (p_{adj}) < 0.05 and $|\log_2$ (FoldChange)| > 0 were considered differentially expressed. Gene Ontology (GO) enrichment analysis of differentially expressed genes and statistical enrichment of differentially expressed genes in KEGG pathways were implemented using the clusterProfiler R package. The differentially expressed genes are listed in Supplementary Table 1. The local version of the GSEA analysis tool (http://www.broadinstitute.org/gsea/index.jsp (accessed on 4 January 2023)) was used for Gene Set Enrichment Analysis (GSEA). GO and the KEGG data set were used for GSEA independently.

RNA isolation and gene expression analysis by RT-qPCR

For total RNA extraction, the NucleoSpin RNA Kit (Macherey-Nagel, Germany) was used according to the manufacturer's recommendations. After RNA isolation, cDNA was synthesized using LunaScript® RT SuperMix Kit (New England Biolabs, MA, USA) by following the manufacturers guidelines. RT-qPCR was performed using Luna® Universal qPCR Master Mix (New England Biolabs, MA, USA) and Rotor-Gene 6000 Real-time PCR system (Corbett Life Science, QIAGEN, Germany) with cycling conditions as follows: 95 ºC 1 min., 95 ºC 15 s, 60 ºC 30 s (40 cycles). The $2^{-\Delta Ct}$ method was used for mRNA quantification analysis [17]. mRNA expression was normalized to the geometric mean of *GAPDH* and *RPL13A* expression. The primer sequences are listed in Supplementary Table S1.

Statistical analysis

IBM SPSS for Windows, version 27.0 (IBM Corp., Armonk, NY, USA) was used for statistical analysis. GraphPad Prism, version 7.0a (GraphPad Software, San Diego, CA, USA) was used for data visualization. Variables are presented as mean ± SD. The Wilcoxon signed-rank test was used to compare time-dependent variables. The paired *t*-test was used to compare related groups. Statistical significance was defined as a two-tailed p-value of ≤ 0.05.

Results

Basic characteristics of the patients

A total of 15 patients, aged 28 to 56 years, with mine-explosive injuries to the lower limbs were enrolled in this study after providing written informed consent. Detailed patient characteristics are shown in Table 1.

Table 1. Clinical characteristics of patients included in this study.

Parameter			*p* value
	Control group (*n* = 7)	**MSC group (*n* = 8)**	
Age (years), mean (range)	39.86 (22–50)	39.5 (28–56)	0.948
Type of injury*, n (%)			
Type 1	0	0	
Type 2	2/7 (28.57%)	5/8 (62.5 %)	
Type 3A	1/7 (14.29%)	2/8 (25 %)	
Type 3B	4/7 (57.14 %)	1/8 (12.5 %)	
Side of injury:			
Left	2/7 (28.57%)	1/8 (12.5%)	
Right	4/7 (57.14%)	7/8 (87.5%)	
Both	1/7 (14.28%)		
Limb fixation device:			
External	4/7 (57.14%)	5/8 (62.5%)	
Internal	0/7 (0.0%)	0/8 (0.0%)	
Without device	3/7 (42.86%)	3/8 (37.5%)	
VAC-therapy:			
Applied	3/7 (42.85%)	4/8 (50%)	
Not applied	4/7 (57.14 %)	4/8 (50 %)	
Skin flap transplantation:			
Performed	6/7 (85.7%)	7/8 (85.7%)	
Not performed	1/7 (12.5%)	1/8 (12.5%)	
Transplant engraftment	6/7 (100 %)	7/8 (100 %)	
Yes	0/7 (0.0 %)	0/8 (0.0 %)	
No			
Self-healing	1/7 (12.5%)	1/8 (12.5%)	
Bed days, mean	73.86	79.0	0.812
Days to transplantation, mean	35.28	24.37	0.121

Bacterial load, CFU×10^6, mean	0.111	5.548	0.606

*: Type 1: clean wound, low-energy puncture wound less than 1 cm, minimal contamination, minimal soft tissue damage, adequate soft tissue coverage of bone, no periostal stripping, minimal fracture fragmentation.

Type 2: moderate soft tissue damage and crushing, moderate contamination, laceration greater than 1 cm, adequate soft tissue coverage of bone, no periosteal stripping, minimal fracture comminution.

Type 3A: high-energy open trauma with a wound area of 100 cm^2 to 600 cm^2, massive wound contamination, extensive soft tissue damage and crushing, adequate soft tissue coverage of bone, severely comminuted and/or segmental fracture, and periosteal detachment.

Type 3B: highly contaminated wound with an area of 100 cm^2 to 600 cm^2, extensive soft tissue damage, inability to cover bone with soft tissue (requiring graft reconstruction), severely comminuted and/or segmental fracture, periosteal stripping, and exposure of bone.

The mean baseline bacterial load (CFU) on the day of admission was 5.548×10^6 in the MSC group and 0.111×10^6 in the control group. During the observation period, the MSC group demonstrated a 4.85-fold decrease in the number of viable microorganisms (mean change: 1.145×10^6 CFU; p = 0.3), whereas the control group showed a 9.8-fold increase (mean change: 1.091×10^6 CFU). No statistically significant differences were observed between the groups at baseline or at the end of the follow-up period.

Effect of hUC-MSCs therapy on the healing of mine explosive wounds

The relative wound area gradually decreased in both groups throughout the observation period (Fig. 1A). The wound healing rate (WHR) in the control group (n=7) was 20.2 % per week. In contrast, in the MSC group (n=8) it was 25.9 % per week. However, no significant difference between the groups was observed (p=0.513) (Fig.1B). Representing images of patients' wounds treated with conventional or MSC therapy are shown in Fig.2. The safety of the hUC-MSCs application was assessed by monitoring adverse events (AEs) recorded within 24 h after treatment, including changes in skin color and measurements of the patient's blood pressure, body temperature, and pulse. Evaluation of potential side effects was performed from the time of administration until the end of the study.

Effect of hUC-MSCs injection on the transcriptome of mine-explosive wounds

We investigated the transcriptomic profiles of wound biopsy samples obtained from patients with mine-explosive injuries of the extremities 24 hours and 7 days after multiple injections of hUC-MSCs.

Bioinformatic analysis of RNA-seq data revealed that 2,304 genes were differentially expressed in the MSC (n=8) group compared with the control (n=7) group ($p_{\text{-value}} \leq 0.05$, $|\log_2 FC| \geq 0$) 24 h after treatment (Fig. 3, Supplementary Table. S2). Among the differentially expressed genes (DEG, $p_{adj} \leq 0.05$), several immune-associated genes were identified. Specifically, increased expression was observed for *MS4A2, TPSB2, CPA3, TPSAB1*. In contrast, decreased expression was detected for *HLA-DQB1, HELZ2, ACOD1, MFSD2B, AIM2, IGLV1-40, HIST1H2AC, MX1, CCL5* (Fig. 3). Furthermore, a downregulation of T cell- and myeloid/macrophage-associated genes was observed in the MSC group compared to the control group (Supplementary Fig. S1).

Gene ontology (GO) analysis of 840 up-expressed (UP) DEGs and 1464 down-expressed (DW) DEGs was performed. According to the GO biological processes database, the most highly expressed UP genes in the MSC group compared with the control group 24 h after treatment were associated with blood circulation and muscle contraction (Fig. 4A). GO biological process analysis showed that genes involved in the regulation of response to biotic stimulus, regulation of innate immune response, defense response to virus and symbiont, positive regulation of defense response, immune response-regulating signaling pathway, positive regulation of response to biotic stimulus, and immune response-activating signaling pathway were downregulated (Fig. 4B).

GO molecular function enrichment analysis of upregulated genes revealed that immunoglobulin complex, monoatomic ion channel complex, and collagen-containing extracellular matrix were the most significantly overrepresented. Among downregulated genes, the most relevant categories were secretory granule membrane, phagocytic vesicle, secretory granule lumen, cytoplasmic vesicle lumen, vesicle lumen (Fig. 4A, B).

KEGG pathway analysis revealed that, 24 h after treatment, the upregulated genes in the MSC group were enriched in pathways related to hypertrophic cardiomyopathy, vascular smooth muscle contraction, cAMP, and cGMP-PKG signaling (Fig. 4C). In contrast, downregulated enriched categories analyzed by KEGG included genes associated with the immune system, especially influenza A, inflammatory bowel disease, measles, osteoclast differentiation, Epstein-Barr virus infection, neutrophil extracellular trap formation, Th17/Th1/Th2 cell differentiation, NOD-like receptor, cytosolic DNA-sensing, Toll-like receptor, JAK-STAT, RIG-I-like receptor, TNF, IL-17, NF-kappa B signaling pathways, indicating the suppression of immune and inflammatory responses in mine-explosive wounds (Fig. 4D).

It was observed that 2,376 genes exhibited altered expression levels in the MSC group (n=7) compared with the control (n=6) group ($p_{value} \leq 0.05$, $|\log_2 FC| \geq 0$) at 7 days after cell therapy (Fig. 5A, B, Supplementary Table S2). Among the DEG we identified a subset of immune associated genes (Fig. 5B, Supplementary Fig. S2). The most relevant upregulated genes ($p_{adj} \leq 0{,}05$) were *QPCT, TIFAB, CCR8, HMOX1, CLEC5A, CCL22, MRC1, CCL24, MS4A2, CPA3, IGHG3, TPSB2, MMP12, CD1B, TPSAB1, TPSD1,*

ADCYAP1, *IGHV5-10-1*, whereas downregulated genes included *PDZK1IP1, CLIC3, VIPR1, CRLF1, CYP2E1, MPP7, KLF4* (Fig. 5B). GO analysis of 770 up-expressed DEGs and 1606 down-expressed DEGs was performed. According to the GO biological processes database, the most highly expressed UP genes in the MSC group compared with the control group 7 days after treatment were involved in cell chemotaxis, leukocyte chemotaxis, leukocyte migration, chemokine-mediated signaling pathway, and response to chemokine (Fig. 6A). In contrast, GO biological process analysis showed that genes involved in cytoplasmic translation and rRNA metabolic process were significantly downregulated (Fig. 6B).

GO molecular function analysis showed that, among upregulated genes, the most relevant categories were cytokine receptor binding and immune and chemokine receptor activity (Fig. 6A). Among downregulated genes, the most pertinent categories were structural constituent of ribosome and rRNA binding (Fig. 6B). KEGG pathway analysis revealed that, 7 days after treatment, upregulated genes in the MSC group were enriched in cytokine-cytokine receptor interaction, viral protein interaction with cytokine and cytokine receptor, chemokine signaling, osteoclast differentiation, vascular smooth muscle contraction, cGMP-PKG, Toll-like receptor, and cAMP signaling pathways (Fig. 6C). KEGG analysis of DW genes in the MSC group compared with the control showed extracellular matrix (ECM) receptor interaction (Fig. 6D). These results indicate that hUC-MSCs therapy has a significant impact on the transcriptome of cells in mine-blast wounds, particularly affecting processes related to the immune system, blood circulation, and muscle function.

A total of 5,161 genes were differentially expressed in the MSC group 24 h after hUC-MSCs treatment ($p_{value} \leq 0.05$, $|\log_2 FC| \geq 0$). Among the most significant DEGs ($p_{adj} \leq 0{,}05$), 432 were upregulated and 1264 were downregulated (Supplementary Table S2). It should be noted that in the control group 1189 genes were differentially expressed ($p_{value} \leq 0.05$, $|\log_2 FC| \geq 0$) at the same time points; of which only 32 were upregulated and 2 were downregulated, ($p_{adj} \leq 0{,}05$) (Supplementary Fig.S3, Supplementary Table S2). Interestingly, according to the GO biological processes database and KEGG analysis, the most significantly upregulated genes 24 h after hUC-MSCs injections were involved in muscle contraction and oxidative phosphorylation (Supplementary Fig.S4A, C). Genes associated with epidermis and skin development, as well as immune system regulation, were enriched within downregulated. DW genes involved in sphingolipid, IL-17, NF-kappa B, and TNF signaling pathways were clustered by KEGG analysis 24 h after hUC-MSCs injection, indicating anti-inflammatory effects of MSC therapy in mine-explosive wounds (Supplementary Fig.S4 B, D).

At 7 day of observation, 2,100 and 1,898 genes were differentially expressed in the MSC and control groups, respectively ($p_{value} \leq 0.05$, $|\log_2 FC| \geq 0$) compared to the day of admission. Among the most significant DEGs ($p_{adj} \leq 0.05$), 25 and 13 genes were upregulated, whereas 299 and 6 genes were downregulated in the MSC and control groups, respectively (Supplementary Table S2). hUC-MSCs injection leads to the suppression of genes involved in skin and epidermis development over the 7-day observation period (Supplementary Fig. S4, S6).

Effect of hUC-MSCs on macrophages in vitro: phagocytosis and gene expression

hUC-MSCs slightly increased the phagocytic activity of peripheral blood monocytes ($CD14^+$)-derived macrophages from patients with mine-explosive wounds in a transwell co-culture model (Fig. 7A, B). RT-qPCR analysis revealed that hUC-MSCs in this model significantly downregulated the expression of the following inflammation-associated genes in macrophages: *KLF4, ACOD1, TIFAB, HMOX1, CLEC5A, PDZK1IP1, IL1B, CXCL10, CCL22, IL10, CXCL8,* and *PTGS2* (Fig. 7C). Some of these genes, such as *KLF4, ACOD1,* and *PDZK1IP1,* were also downregulated in mine explosive wounds after cell therapy compared with the control group. Changes in *CLEC5A, CXCL8,* and *PTGS2* expression in macrophages under hUC-MSCs influence were consistent with the alterations observed in wound tissues 24 h after cell injection. In contrast, the expression of *AIM2, MX1, MMP12, CCL17, CSF3,* and *CD1B* was not affected in the co-culture system, whereas all these genes were upregulated in wound tissues 7 days after cell therapy. Furthermore, *CXCL8* expression was downregulated in macrophages co-cultured with hUC-MSCs but remained unchanged in wounds tissues following cell therapy.

Effect of hUC-MSCs on CD4+ T cells in vitro: proliferation, immunophenotype, and gene expression

hUC-MSCs significantly suppressed the proliferative activitiy of $CD4^+$ T cells isolated from PBMC of patients with mine-explosive wounds (Fig. 8A). Flow cytometry analysis demonstrated a significant increase in early activated $CD4^+CD69^+CD25^+CD127^+$ cells among $CD4^+$ T cells after co-culture with hUC-MSCs. Furthermore, there was a tendency to increased proportions of $CD127^+$ (p=0.058), $CD69^+CD25^+$ (p=0.069) and $CD4^+CD25^{low}CD127^{low}$ (p=0.069) cell subpopulations among $CD4^+$ T cells following co-culture with hUC-MSCs. hUC-MSCs did not affect the maturation of Th cells ($CD183^+$), senescent effector of Th cells ($CD57^+183^+$), and memory Th cells ($CD57^+183^+CD45RO^+$) (Fig. 8B). Expression levels of *CD70* and *HLA-DQB1* tended to decrease in $CD4^+$ T cells after co-culturing with hUC-MSCs, whereas genes including *TNFAIP2, IL6, CXCL8, CCL5, IFNG, CD160,* and *CXCR2* were not markedly altered (Fig. 8C).

Effect of hUC-MSCs on PBMC in vitro: proliferation and immunophenotype

Co-culture with hUC-MSCs significantly decreased the proliferation of PBMC from patients with mine-explosive wounds (Fig. 9A). Following co-culture with hUC-MSCs, the percentage of $CD14^+$ monocytes with M2-like phenotype $CD14^+CD206^+$, $CD14^-CD80^+$ cells, and $CD4^+$ T-helpers were increased among $CD45^+$ cells, whereas the percentage of total $CD8^+$ cells, exhausted $CD4^+$ T cells ($CD4^+CD57^+CD279^+$),

and exhausted $CD8^+$ T cells ($CD8^+CD57^+CD279^+$) were decreased (Fig. 9B). These results indicate that hUC-MSCs exert anti-inflammatory properties in the co-culture model.

Discussion

In the present study, we aimed to investigate the impact of human umbilical cord-derived mesenchymal stromal cell transplantation on the safety and clinical outcomes of patients with mine-explosive wounds, with a focus on transcriptomic profile changes in the wounds and the efficiency of complex surgical treatment. The administration of hUC-MSCs was safe and was not associated with adverse events or alterations in the rate of clinical healing during a week observation period. Engraftment of free TFL flaps and non-vascularized autologous skin grafts was observed in all patients.

RNA-seq analysis revealed that hUC-MSCs injections induced a pronounced short-term anti-inflammatory effect in wounds, which was no longer detectable by the 7th day. The reduction in the expression levels of *KLF4, ACOD1, PDZK1IP1, CLEC5A, CXCL8*, and *PTGS2* genes in macrophages co-cultured with hUC-MSCs mirrored the changes observed in wounds 24 h after cell injection. Previous studies have demonstrated that *KLF4* plays a critical role in mediating proinflammatory responses in macrophages, and its downregulation under the influence of anti-inflammatory growth factor TGF-β1 promotes M2 phenotype [18, 19]. Moreover, *KLF4* expression supports cutaneous wound healing in mice and the expansion of keratinocyte precursors from adult human skin [20, 21]. Activation of macrophages by different pathogen infections and pathogen-associated molecular pattern molecules, as well as cytokines (e.g., TNF and IFNs), leads to upregulation of *ACOD1* expression [22].

PDZK1IP1 plays an essential role in the inflammatory phenotype in tumors and other inflammatory conditions, including psoriasis. Furthermore, PDZK1IP1 was found to directly regulate NFAT2 and IL-6 activation, inducing the differentiation of monocytes into dendritic cells [23]. The surface expression of *CLEC5A* is highest on proinflammatory M1 macrophages, while intermediate on M2 macrophages, and its activation by pathogen-derived antigens induces the secretion of proinflammatory mediators [24]. *CXCL8* and *PTGS2* expressions are rapidly upregulated in wounds, reaching levels significantly higher than in normal tissue [25, 26]. *CXCL8* is a chemokine that is increasingly expressed in macrophages under inflammatory conditions [27]. However, in our co-culture system we observed the downregulation of *PTGS2* under the influence of hUC-MSCs, which contrasts with its anti-inflammatory role in M2 macrophages [28]. Therefore, the reduced expression of *KLF4, ACOD1, PDZK1IP1, CLEC5A, CXCL8*, and *PTGS2* genes in mine-explosive wounds on day 1 and in macrophages in the co-culture system may reflect their important role in the anti-inflammatory effect of UC-MSC.

It was reported that MSC-conditioned media treatment inhibited IL1β mRNA transcription in LPS-stimulated macrophages [29], which is consistent with our experimental findings. It was shown that the expression of inflammatory genes *MX1* and *AIM2* in wounds was downregulated on day 1 after cell therapy, unlike in macrophages. Immune cell infiltration analysis revealed that *MX1* was associated with M1 macrophage [30]. *AIM2* expression is strongly upregulated in inflamed skin [31]. The downregulation

of inflammation-associated genes in macrophages co-cultured with hUC-MSCs and stimulation of phagocytosis suggested a shift toward an anti-inflammatory phenotype [32–34]. Furthermore, the increasing frequency of monocytes expressing the M2 macrophage marker CD206 in the hUC-MSCs/PBMCs co-culture system confirms the anti-inflammatory properties of MSCs [35].

The expression levels of *CD70* and *HLA-DQB1* decreased in $CD4^+$ T cells after co-culture with hUC-MSCs, consistent with *in vivo* RNA-Seq data from wounds 1 day after cell therapy. In contrast, the expression patterns of *TNFAIP2, CD1B, IL6, CXCL8, CCL5, IFNG, CD160*, and *CXCR2* differed between wounds and $CD4^+$ T cells under the influence of hUC-MSCs. The immune system in wounds represented a highly complex network comprising various immune cell types, such as T, B, NK, innate lymphoid cells, macrophages, dendritic cells, and neutrophils [13, 36]. The multitarget effect of hUC-MSCs *in vivo* may explain the observed differences in immune gene expression between macrophages *in vitro* and wounds.

In this study, we demonstrated that hUC-MSCs significantly inhibited the proliferative activity of $CD4^+$ T cells isolated from peripheral blood of patients with mine-explosive wounds. Moreover, a reduction in the pool of effector T cells after co-culturing activated PBMCs with hUC-MSCs has been reported previously [15, 35]. Our study shows that hUC-MSCs induce the expression of CD69, an early T cell activation marker, and CD25 as a mid-stage marker, consistent with prior studies [15, 37, 38]. Furthermore, the increased proportion of $CD69^+$ T-reg cells among $CD4^+$ T cells under hUC-MSCs co-culture in our research suggests their anti-inflammatory properties, as previously described [39]. The decrease in the $CD4^+/CD8^+$ cells ratio and in exhausted T cell subsets under hUC-MSCs treatment of PBMCs suggested an anti-inflammatory effect on T cells, in agreement with existing literature [15, 40].

Interestingly, hUC-MSCs therapy upregulated several immune-associated genes one week after treatment, including *TIFAB, HMOX1, CLEC5A, MRC1, MMP12, CD1B, CCL22, CCL17, CSF3, CCL24*, and *CCR8*. Given that *MRC1, CCL22, CCL17, CCL24, CCR8*, *CSF3*, and *MMP12* are markers of M2 macrophages [41–43], their increased expression in the wound could suggest anti-inflammatory effects of hUC-MSCs on mine-explosive wound healing. Furthermore, the hUC-MSCs have been shown to upregulate *MRC1, CCL22, CCL24, CLEC5A*, and *CSF3* in PBMC from COVID-19 patients under co-culture conditions [15]. In contrast to anti-inflammatory effects on wounds, we observed upregulation of mast-associated genes *ADCYAP1, CPA3, TPSAB1, TPSB2, TPSD1*, and *MS4A2* on days 1 and 7 after therapy. The elevation of both mast- and macrophage M2-associated genes may reflect an MSC-induced type 2-like immune response in wounds. Mast cells play a crucial role in routine wound healing but are also associated with excessive scarring [44, 45].

It has been previously demonstrated that xenogeneic mesenchymal stromal cells enhance wound healing and exhibit immunosuppressive effects in a rat model of extensive burn [46]. Treatment of skin wounds with bone-marrow MSC-conditioned medium (BM-MSC CM) also led to increased neutrophil and macrophage infiltration. Chronic methicillin-resistant *Staphylococcus aureus*-infected wounds treated with BM-MSC CM showed a reduced bacterial load accompanied by better resolution of granulation tissue formation and increased infiltration of pro-healing M2 macrophages compared with control-

treated infected wounds [47]. In this study, we demonstrated for the first time the anti-inflammatory effect of hUC-MSCs on wounds in humans at the transcriptome level, consistent with results from non-clinical studies.

Mitochondrial genes involved in oxidative phosphorylation, including *NDUFA11, MT-ND1, NDUFV1, MT-CYB, MT-ND4L, MT-ND2, NDUFS8, NUPR1, MT-ND5, MT-CO3, MT-CO1, MT-ND6, MT-CO2, MT-ND4* and *MT-ATP6* were significantly upregulated after hUC-MSCs therapy. In contrast, chronic and acute wounds exhibited significant downregulation of the *MT-CYB, MT-ND4L, MT-ATP8, MT-ND4, MT-ND5, MT-CO3, MT-ATP6, MT-CO1, MT-ND1*, and *MT-CO2* genes compared to normal skin [48]. The upregulation of OXPHOS-associated genes in wounds reflects accelerated healing processes [49]. However, elevated expression of *MT-ND1, MT-ND4, MT-ND5*, and *MT-CO1* in chronic wounds can lead to increased ROS production during mitochondrial respiration, contributing to high levels of oxygen species in chronic wounds [50]. The ROS-involved genes (*DUOX1, SOD2*) were downregulated in wounds after hUC-MSCs therapy, suggesting that the elevation of OXPHOS-associated genes is linked to aerobic respiration rather than to ROS production, which is consistent with attenuation of inflammation.

The anti-inflammatory effects associated with hUC-MSCs injection were accompanied by downregulation of genes involved in skin and epidermis development, including *FGF22, SPTSSB*, and *FGFR2*. We propose that this effect may be related to the suppression of wound inflammation. It is known that anti-inflammatory therapy delays wound healing [51–53]. hUC-MSCs-mediated immunosuppression could inhibit re-epithelialization, which requires pro-inflammatory macrophages during the inflammatory phase of wound regeneration [36]. Furthermore, comparison with single-cell data from venous and diabetic foot ulcers reveals a connection between impaired keratinocyte migration and an inadequate inflammatory response in chronic wounds [47, 48].

Conclusion

In the present study, we demonstrated that hUC-MSCs transplantation was safe and did not affect the healing rate of mine-explosive wounds in humans within one week. The engraftment of free flaps and non-vascularized autologous skin grafts could benefit from the anti-inflammatory effect of hUC-MSCs on wounds in complex surgical treatment of mine-explosive wounds. Observed gene expression changes in macrophages, $CD4^+$ T cells, and PBMCs highlight the potency of hUC-MSCs to attenuate inflammation in mine-explosive wounds at the transcriptomic level. The challenge of determining the long-term effects, including their impact on reconstructive outcomes, systemic immune response, and long-term tissue quality, remains to be addressed through further randomized controlled trials.

Abbreviations

MSCs – mesenchymal stromal cells

hUC-MSCs – human umbilical cord-derived MSCs

RT-qPCR – real time quantitative polymerase chain reaction

UCs – umbilical cords

SAEs – serious adverse events

WA – wound area

PBMC – peripheral blood mononuclear cells

WHR – wound healing rate

DEGs – differentially expressed genes

Declarations

Availability of data and materials

The datasets supporting the conclusions of this article are included within the article and its additional files.

Funding

The project “Molecular mechanisms of the therapeutic effect of the transplantation of placental mesenchymal stromal cells in the treatment of mine-explosive injuries of the lower limbs in humans” was funded from the state budget and implemented under the cooperation programme between the Ministry of Education, Science and Sport of the Republic of Lithuania, Research Council of Lithuania (project registration No. P-LU-24-86, grant No. S-LU-24-10) and the Ministry of Education and Science of Ukraine (№ 0225U004555).

Authors' contributions

V.S., A.U., Y.S., V.B., R.N. – conceived and designed the study, administrating and managing research, wrote and revised the manuscript; V.S – performed bioinformatics analysis of RNAseq; E.V., G.V., D.Š., A.Z., V.B.– performed processing and testing; Y.S., R.S. – conceived and designed the study, conducted clinical assessments of patients, administered hUC-MSCs injections, carried out follow-ups; T.B., A.U., I.Z., V.K. – performed processing, testing, and preparation of UC-MSC for transplantation and PBMC/macrophages/T cells co-culture with UC-MSC, performed the measurements and analyzed the data, wrote and revised the manuscript; V.K. – conducted flow cytometry analysis; I.S. – administrating and managing research. All authors contributed to the manuscript and approved the submitted version. All authors have read and agreed to the published version of the manuscript.

Volodymyr Shablii and Rūta Navakauskienė are the corresponding authors.

Acknowledgement

The authors express their gratitude to S. Martynenko, the director of the Institute of Cell Therapy, for helping to organize and for supporting this research. The authors acknowledge the Armed Forces of Ukraine for their service and for enabling the medical care, research and clinical conditions under which this work became possible. We also acknowledge all medical personnel involved in the treatment of patients included in this study. The authors declare that they have not use AI-generated work in this manuscript.

Ethics declarations

Ethics approval and consent to participate

The protocol of this study entitled “Molecular mechanisms of the therapeutic effect of the transplantation of placental mesenchymal stromal cells in the treatment of mine explosive injuries of the lower limbs in humans” and the consent procedure were approved by the Committee of Human Research of the Institute of Cell Therapy (No.01-24, January 17, 2024) and by the Vilnius Regional Biomedical Research Ethics Committee (protocol No. P-5/2024, version No. V-5/2024, 07 October, 2024).

In addition, the protocol of the prospective, single-center, open-label, non-randomized study was developed in accordance with the Declaration of Helsinki and approved by the local Ethics Committee of the O.O. Shalimov National Scientific Center of Surgery and Transplantology (Protocol No. 10/05/2024, May 10, 2024). Due to the exploratory and pilot nature of the study, it was not registered in a public clinical trial registry. All participants enrolled in the clinical trial and who provided biological material for this study signed informed consent statements.

Consent for publication

Not applicable.

Competing interests

The authors declare that they have no competing interests.

References

1. Ukraine. accessed December 11, : AOAV explosive violence data on harm to civilians (Last updated: 10 July 2025) - Ukraine | ReliefWeb n.d. https://reliefweb.int/report/ukraine/ukraine-aoav-explosive-violence-data-harm-civilians-last-updated-10-july-2025 (2025).
2. Lawry LL, Mani V, Hamm TE, Janvrin M, Juman L, Korona-Bailey J, et al. Qualitative assessment of combat-related injury patterns and injury prevention in Ukraine since the Russian invasion. BMJ Mil Health. 2025;0:1–6. https://doi.org/10.1136/MILITARY-2024-002863.
3. How many Ukrainian soldiers have died?. n.d. https://www.economist.com/graphic-detail/2024/11/26/how-many-ukrainian-soldiers-have-died (accessed December 11, 2025).

4. Hwang JJ, Rim YA, Nam Y, Ju JH. Recent Developments in Clinical Applications of Mesenchymal Stem Cells in the Treatment of Rheumatoid Arthritis and Osteoarthritis. Front Immunol. 2021;12:631291. https://doi.org/10.3389/FIMMU.2021.631291/XML.
5. Cao M, Ou Z, Sheng R, Wang Q, Chen X, Zhang C, et al. Efficacy and safety of mesenchymal stem cells in knee osteoarthritis: a systematic review and meta-analysis of randomized controlled trials. Stem Cell Res Therapy. 2025;16:122. https://doi.org/10.1186/S13287-025-04252-2/FIGURES/8.
6. Fernández-Francos S, Eiro N, González-Galiano N, Vizoso FJ. Mesenchymal Stem Cell-Based Therapy as an Alternative to the Treatment of Acute Respiratory Distress Syndrome: Current Evidence and Future Perspectives. Int J Mol Sci 2021. 2021;22:22. https://doi.org/10.3390/IJMS22157850.
7. Holiuk Y, Birsa R, Bukreieva T, Nemtinov P, Kyryk V, Ustymenko A, et al. Effectiveness and safety of multiple injections of human placenta-derived MSCs for knee osteoarthritis: a nonrandomized phase I trial. BMC Musculoskelet Disord. 2025;26:418. https://doi.org/10.1186/s12891-025-08664-2.
8. Guillamat-Prats R, Guillamat-Prats R. The Role of MSC in Wound Healing, Scarring and Regeneration. Cells 2021, 10, 2021;10. https://doi.org/10.3390/CELLS10071729
9. Otero-Viñas M, Falanga V. Mesenchymal Stem Cells in Chronic Wounds: The Spectrum from Basic to Advanced Therapy. Adv Wound Care (New Rochelle). 2016;5:149–63. https://doi.org/10.1089/WOUND.2015.0627.
10. Shu X, Shu S, Tang S, Yang L, Liu D, Li K, et al. Efficiency of stem cell based therapy in the treatment of diabetic foot ulcer: a meta-analysis. Endocr J. 2018;65:403–13. https://doi.org/10.1507/ENDOCRJ.EJ17-0424.
11. Prokopenko KA, Parkhomenko KYu, Dudchenko MO, Kravtsiv MI, Drozdova AH. Improving surgical strategies for treating extensive soft tissue wounds resulting from mine and explosive trauma. Stomatological Academy]. 2023;23:159–62. https://doi.org/10.31718/2077-1096.23.4.159. Актуальні Проблеми Сучасної Медицини: Вісник Української Медичної Стоматологічної Академії [Current Problems of Modern Medicine: Bulletin of the Ukrainian Medical.
12. Connolly M, Ibrahim ZR, Iii ONJ. Changing paradigms in lower extremity reconstruction in war-related injuries 2016. https://doi.org/10.1186/s40779-016-0080-7
13. Kravtsov OV, Klimova EM, Drozdova LA. Dynamics of changes in immunological indicators during surgical and local treatment of soft tissue defects in mine-blast injury. Kharkiv Surg School 2025:92–7. https://doi.org/10.37699/2308-7005.1.2025.15
14. Masson-Meyers DS, Tayebi L. Vascularization strategies in tissue engineering approaches for soft tissue repair. J Tissue Eng Regen Med. 2021;15:747–62. https://doi.org/10.1002/TERM.3225.
15. Bukreieva T, Svitina H, Nikulina V, Vega A, Chybisov O, Shablii I, et al. Treatment of Acute Respiratory Distress Syndrome Caused by COVID-19 with Human Umbilical Cord Mesenchymal Stem Cells. Int J Mol Sci. 2023;24:4435. https://doi.org/10.3390/IJMS24054435/S1.
16. Dominici M, Le Blanc K, Mueller I, Slaper-Cortenbach I, Marini F, Krause D, et al. Minimal criteria for defining multipotent mesenchymal stromal cells. The International Society for Cellular Therapy

position statement. Cytotherapy. 2006;8:315–7. https://doi.org/10.1080/14653240600855905.

17. Livak KJ, Schmittgen TD. Analysis of relative gene expression data using real-time quantitative PCR and the 2(-Delta Delta C(T)) Method. Methods. 2001;25:402–8. https://doi.org/10.1006/meth.2001.1262.
18. Herta T, Bhattacharyya A, Hippenstiel S, Zahlten J. The role of KLF4 in phagocyte activation during infectious diseases. Front Immunol. 2025;16:1584873. https://doi.org/10.3389/FIMMU.2025.1584873/BIBTEX.
19. Feinberg MW, Cao Z, Wara AK, Lebedeva MA, SenBanerjee S, Jain MK. Kruppel-like Factor 4 Is a Mediator of Proinflammatory Signaling in Macrophages. J Biol Chem. 2005;280:38247–58. https://doi.org/10.1074/JBC.M509378200.
20. Fortunel NO, Chadli L, Coutier J, Lemaître G, Auvré F, Domingues S, et al. KLF4 inhibition promotes the expansion of keratinocyte precursors from adult human skin and of embryonic-stem-cell-derived keratinocytes. Nat Biomedical Eng 2019. 2019;3:12. https://doi.org/10.1038/s41551-019-0464-6.
21. Ou L, Shi Y, Dong W, Liu C, Schmidt TJ, Nagarkatti P, et al. Kruppel like factor KLF4 facilitates cutaneous wound healing by promoting fibrocyte generation from myeloid-derived suppressor cells. J Invest Dermatol. 2015;135:1425. https://doi.org/10.1038/JID.2015.3.
22. Wu R, Chen F, Wang N, Tang D, Kang R. ACOD1 in immunometabolism and disease. Cell Mol Immunol 2020. 2020;17:8. https://doi.org/10.1038/s41423-020-0489-5.
23. García-Heredia JM, Carnero A. The cargo protein MAP17 (PDZK1IP1) regulates the immune microenvironment. Oncotarget. 2017;8:98580–97. https://doi.org/10.18632/ONCOTARGET.21651.
24. Tosiek MJ, Groesser K, Pekcec A, Zwirek M, Murugesan G, Borges E. Activation of the Innate Immune Checkpoint CLEC5A on Myeloid Cells in the Absence of Danger Signals Modulates Macrophages' Function but Does Not Trigger the Adaptive T Cell Immune Response. J Immunol Res. 2022;2022:1–22. https://doi.org/10.1155/2022/9926305.
25. Ridiandries A, Tan JTM, Bursill CA. The Role of Chemokines in Wound Healing. Int J Mol Sci. 2018;19:3217. https://doi.org/10.3390/ijms19103217.
26. Zhu AS, Li A, Ratliff TS, Melsom M, Garza LA. After Skin Wounding, Noncoding dsRNA Coordinates Prostaglandins and Wnts to Promote Regeneration. J Invest Dermatology. 2017;137:1562–8. https://doi.org/10.1016/j.jid.2017.03.023.
27. Chen S, Saeed AFUH, Liu Q, Jiang Q, Xu H, Xiao GG, et al. Macrophages in immunoregulation and therapeutics. Signal Transduct Target Ther. 2023;8:207. https://doi.org/10.1038/s41392-023-01452-1.
28. Wang W, Liang M, Wang L, Bei W, Rong X, Xu J, et al. Role of prostaglandin E2 in macrophage polarization: Insights into atherosclerosis. Biochem Pharmacol. 2023;207:115357. https://doi.org/10.1016/j.bcp.2022.115357.
29. Jin QH, Kim HK, Na JY, Jin C, Seon JK. Anti-inflammatory effects of mesenchymal stem cell-conditioned media inhibited macrophages activation in vitro. Sci Rep. 2022;12:4754. https://doi.org/10.1038/S41598-022-08398-4.

30. Tian M, Tang M, Chen C, Lin Y, Chen H, Xu Y. Macrophage Infiltration Correlated with IFI16, EGR1 and MX1 Expression in Renal Tubular Epithelial Cells Within Lupus Nephritis-Associated Tubulointerstitial Injury via Bioinformatics Analysis. J Inflamm Res 2024;Volume 17:11469–83. https://doi.org/10.2147/JIR.S489087
31. Sharma BR, Karki R, Kanneganti T. Role of AIM2 inflammasome in inflammatory diseases, cancer and infection. Eur J Immunol. 2019;49:1998–2011. https://doi.org/10.1002/eji.201848070.
32. Holopainen M, Impola U, Lehenkari P, Laitinen S, Kerkelä E. Human Mesenchymal Stromal Cell Secretome Promotes the Immunoregulatory Phenotype and Phagocytosis Activity in Human Macrophages. Cells 2020, Vol 9, Page 2142. 2020;9:2142. https://doi.org/10.3390/CELLS9092142
33. Ko JH, Kim HJ, Jeong HJ, Lee HJ, Oh JY. Mesenchymal Stem and Stromal Cells Harness Macrophage-Derived Amphiregulin to Maintain Tissue Homeostasis. Cell Rep. 2020;30:3806–e38206. https://doi.org/10.1016/j.celrep.2020.02.062.
34. Evans JF, Ricigliano AE, Morante AV, Martinez E, Vargas D, Thyagaraj J. Mesenchymal Stem Cell Regulation of Macrophage Phagocytosis; Quantitation and Imaging. J Vis Exp 2021;2021. https://doi.org/10.3791/62729
35. Cruz-Barrera M, Flórez-Zapata N, Lemus-Diaz N, Medina C, Galindo CC, González-Acero LX, et al. Integrated Analysis of Transcriptome and Secretome From Umbilical Cord Mesenchymal Stromal Cells Reveal New Mechanisms for the Modulation of Inflammation and Immune Activation. Front Immunol. 2020;11:575488. https://doi.org/10.3389/FIMMU.2020.575488/BIBTEX.
36. Liu Z, Bian X, Luo L, Björklund ÅK, Li L, Zhang L, et al. Spatiotemporal single-cell roadmap of human skin wound healing. Cell Stem Cell. 2025;32:479–e4988. https://doi.org/10.1016/j.stem.2024.11.013.
37. Zhu R, Yan T, Feng Y, Liu Y, Cao H, Peng G, et al. Mesenchymal stem cell treatment improves outcome of COVID-19 patients via multiple immunomodulatory mechanisms. Cell Res 2021. 2021;31:12. https://doi.org/10.1038/s41422-021-00573-y.
38. Araujo FS, Panepucci RA, Farias KC, Araujo AG, Orellana MD, Menezes CB, et al. Mesenchymal Stromal Cells Promote a Sustained Increase of the CD69 Marker on Activated CD3 + Lymphocytes: Potential Immunomodulatory Role. Blood. 2008;112:2417. https://doi.org/10.1182/BLOOD.V112.11.2417.2417.
39. Blanco-Dominguez R, De H, Fuente L, Garcia-Guimaraes MM, Rodriguez C, Rodriguez-Arabaolaza I et al. CD69 expression in regulatory T cells protects from the immune-mediated damage after myocardial infarction. Eur Heart J 2021;42. https://doi.org/10.1093/EURHEARTJ/EHAB724.3239
40. Herzig MC, Christy BA, Montgomery RK, Delavan CP, Jensen KJ, Lovelace SE, et al. Interactions of human mesenchymal stromal cells with peripheral blood mononuclear cells in a Mitogenic proliferation assay. J Immunol Methods. 2021;492:113000. https://doi.org/10.1016/j.jim.2021.113000.
41. Shrivastava R, Shukla N. Attributes of alternatively activated (M2) macrophages. Life Sci. 2019;224:222–31. https://doi.org/10.1016/j.lfs.2019.03.062.

42. Karagiannidis I, de Santana Van Vilet E, Said Abu Egal E, Phinney B, Jacenik D, Prossnitz ER, et al. G-CSF and G-CSFR Induce a Pro-Tumorigenic Macrophage Phenotype to Promote Colon and Pancreas Tumor Growth. Cancers (Basel). 2020;12:2868. https://doi.org/10.3390/cancers12102868.
43. Kuntschar S, Cardamone G, Klann K, Bauer R, Meyer SP, Raue R, et al. Mmp12 Is Translationally Regulated in Macrophages during the Course of Inflammation. Int J Mol Sci. 2023;24. https://doi.org/10.3390/ijms242316981.
44. Wilgus TA, Wulff BC. The Importance of Mast Cells in Dermal Scarring. Adv Wound Care (New Rochelle). 2014;3:356. https://doi.org/10.1089/WOUND.2013.0457.
45. Guth C, Limjunyawong N, Pundir P. The evolving role of mast cells in wound healing: insights from recent research and diverse models. Immunol Cell Biol. 2024;102:878–90. https://doi.org/10.1111/IMCB.12824.
46. Caliari-Oliveira C, Yaochite JNU, Ramalho LNZ, Palma PVB, Carlos D, De Queiróz Cunha F, et al. Xenogeneic Mesenchymal Stromal Cells Improve Wound Healing and Modulate the Immune Response in an Extensive Burn Model. Cell Transpl. 2016;25:201–15. https://doi.org/10.3727/096368915X688128.
47. Rajesh A, Ju EDE, Oxford KA, Harman RM, Van de Walle GR. The mesenchymal stromal cell secretome promotes tissue regeneration and increases macrophage infiltration in acute and methicillin-resistant Staphylococcus aureus-infected skin wounds in vivo. Cytotherapy. 2024;26:1400–10. https://doi.org/10.1016/J.JCYT.2024.06.007/ATTACHMENT/3442CBB6-6625-49F9-BF33-AF4DC677E024/MMC3.PPTX.
48. Manchanda M, Torres M, Inuossa F, Bansal R, Kumar R, Hunt M, et al. Metabolic Reprogramming and Reliance in Human Skin Wound Healing. J Invest Dermatology. 2023;143:2039–51. https://doi.org/10.1016/j.jid.2023.02.039. .e10.
49. Hunt M, Torres M, Bachar-Wikström E, Wikström JD. Multifaceted roles of mitochondria in wound healing and chronic wound pathogenesis. Front Cell Dev Biol 2023;11. https://doi.org/10.3389/fcell.2023.1252318
50. Jabbari P, Kim JH, Le BH, Zhang W, Zhang H, Martins-Green M. Chronic Wound Initiation: Single-Cell RNAseq of Cutaneous Wound Tissue and Contributions of Oxidative Stress to Initiation of Chronicity. Antioxidants. 2025;14:214. https://doi.org/10.3390/antiox14020214.
51. Gaber MW, Aziz AM, Shang X, Penmetsa R, Sabek OM, Yen MRT, et al. Changes in Abdominal Wounds Following Treatment With Sirolimus and Steroids in a Rat Model. Transpl Proc. 2006;38:3331–2. https://doi.org/10.1016/j.transproceed.2006.10.047.
52. Busti AJ, Hooper JS, Amaya CJ, Kazi S. Effects of Perioperative Antiinflammatory and Immunomodulating Therapy on Surgical Wound Healing. Pharmacotherapy: J Hum Pharmacol Drug Therapy. 2005;25:1566–91. https://doi.org/10.1592/phco.2005.25.11.1566.
53. Na YR, Yoon YN, Son D, Jung D, Gu GJ, Seok SH. Consistent Inhibition of Cyclooxygenase Drives Macrophages towards the Inflammatory Phenotype. PLoS ONE. 2015;10:e0118203. https://doi.org/10.1371/journal.pone.0118203.

Figures

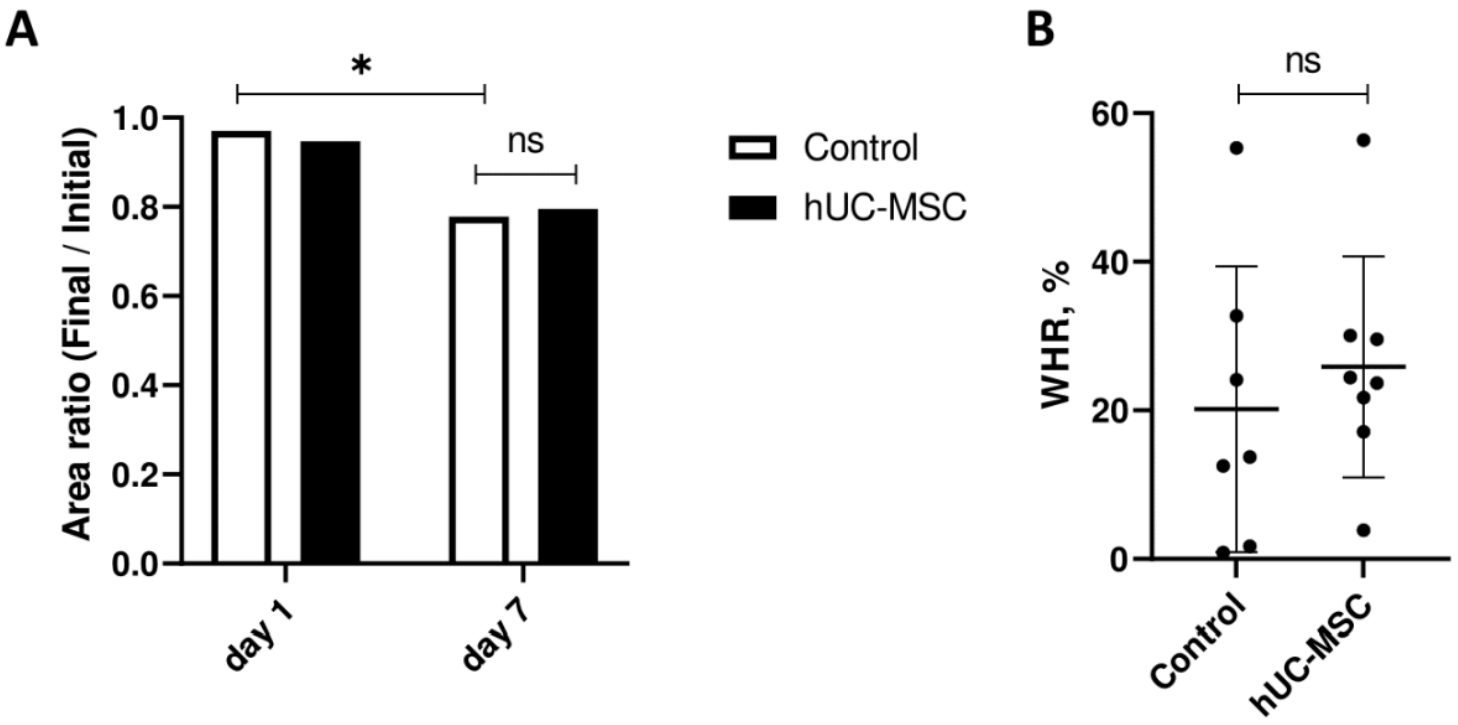


Figure 1

Effect of hUC-MSC therapy on wounds healing. (A) ratio of wound area on day 1 and day 7; (B) wound healing rate. Data are presented as mean ± SD. Statistical comparisons within and between groups were performed using the Wilcoxon signed-rank test. *, $p \leq 0.05$.

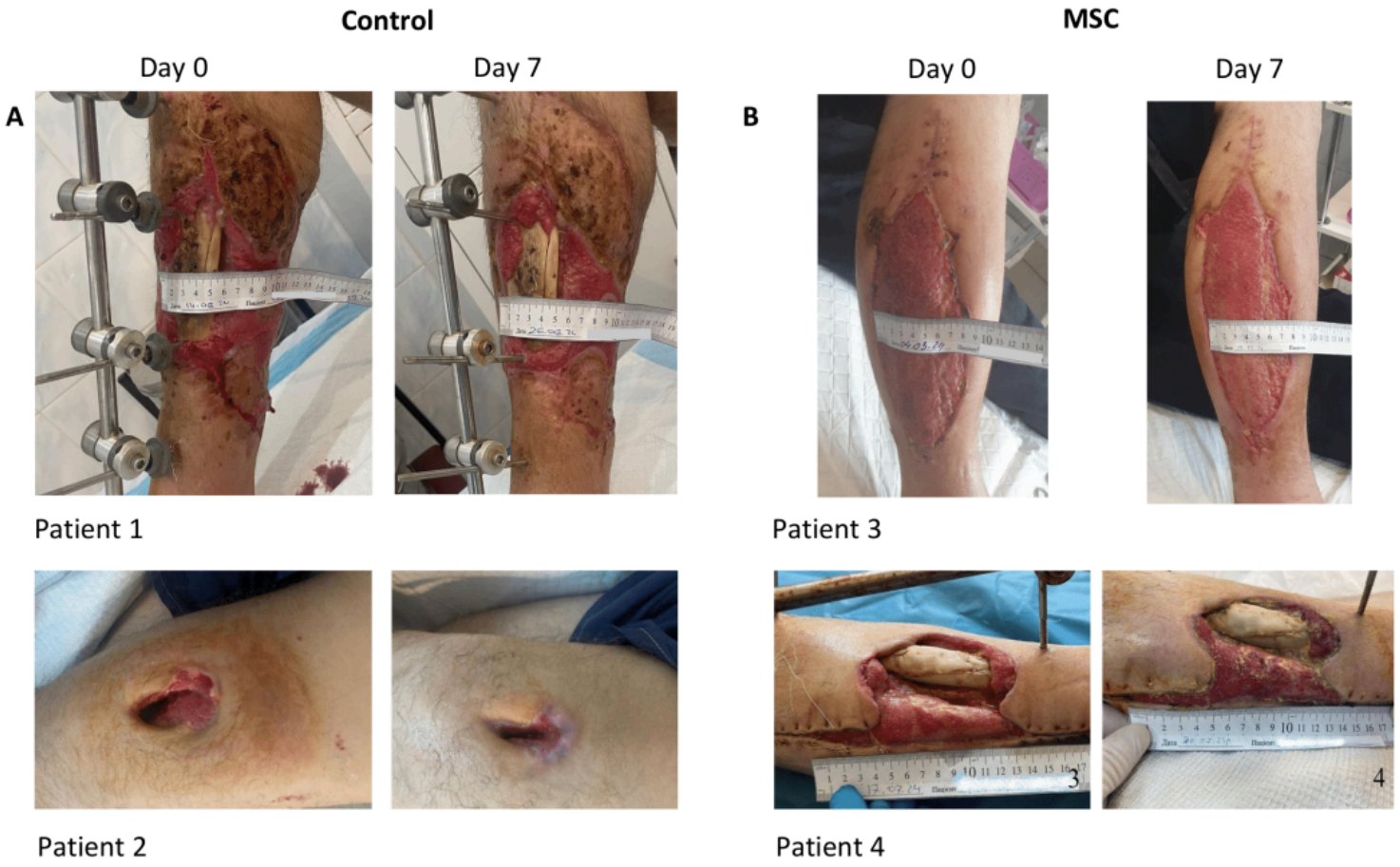


Figure 2

Representative images of wounds in the control (A) and MSC (B) groups on a day 0 and day 7.

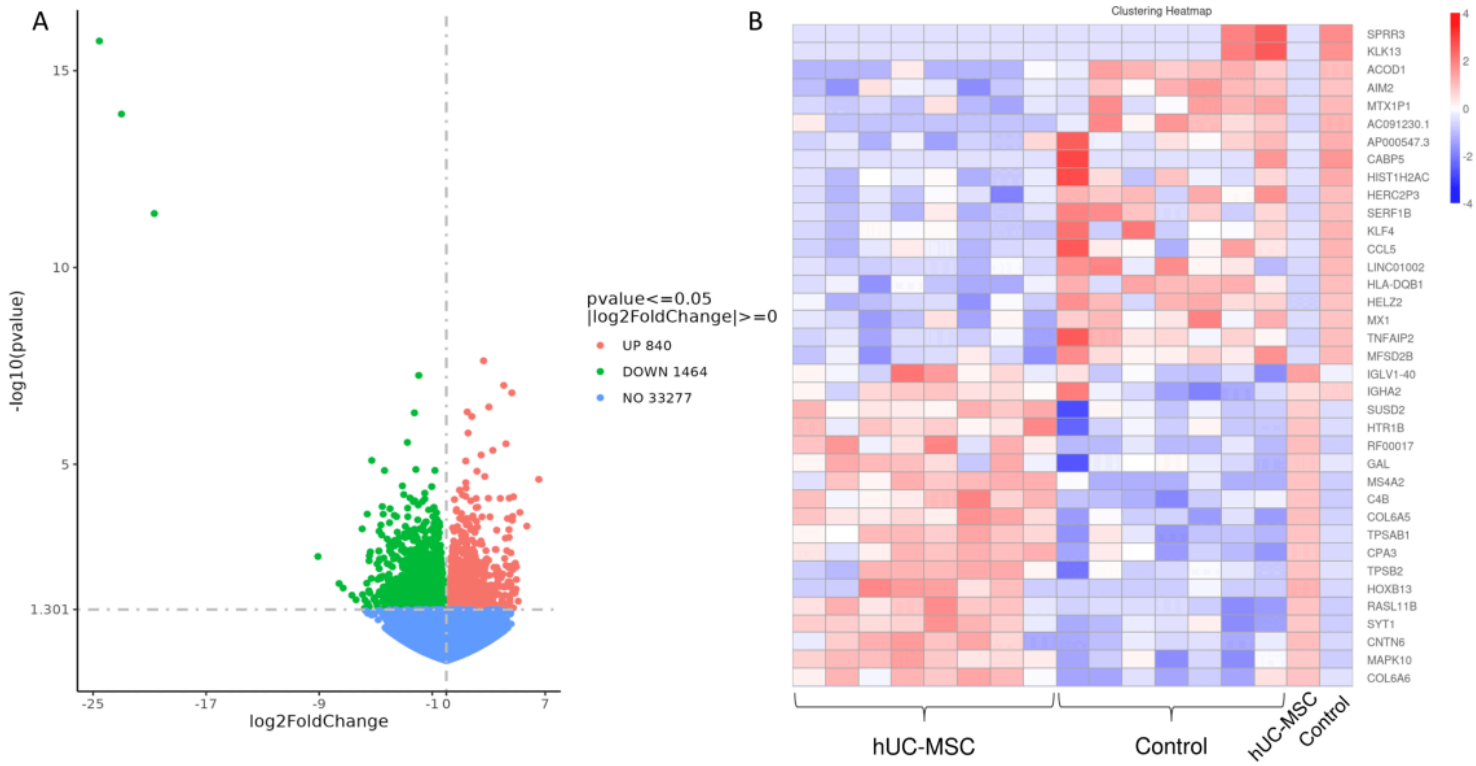


Figure 3

Differentially expressed genes (DEGs) in the MSC and the control groups 24 h after hUC-MSCs injections. A) Volcano plot of DEGs; B) Heatmap of DEGs.

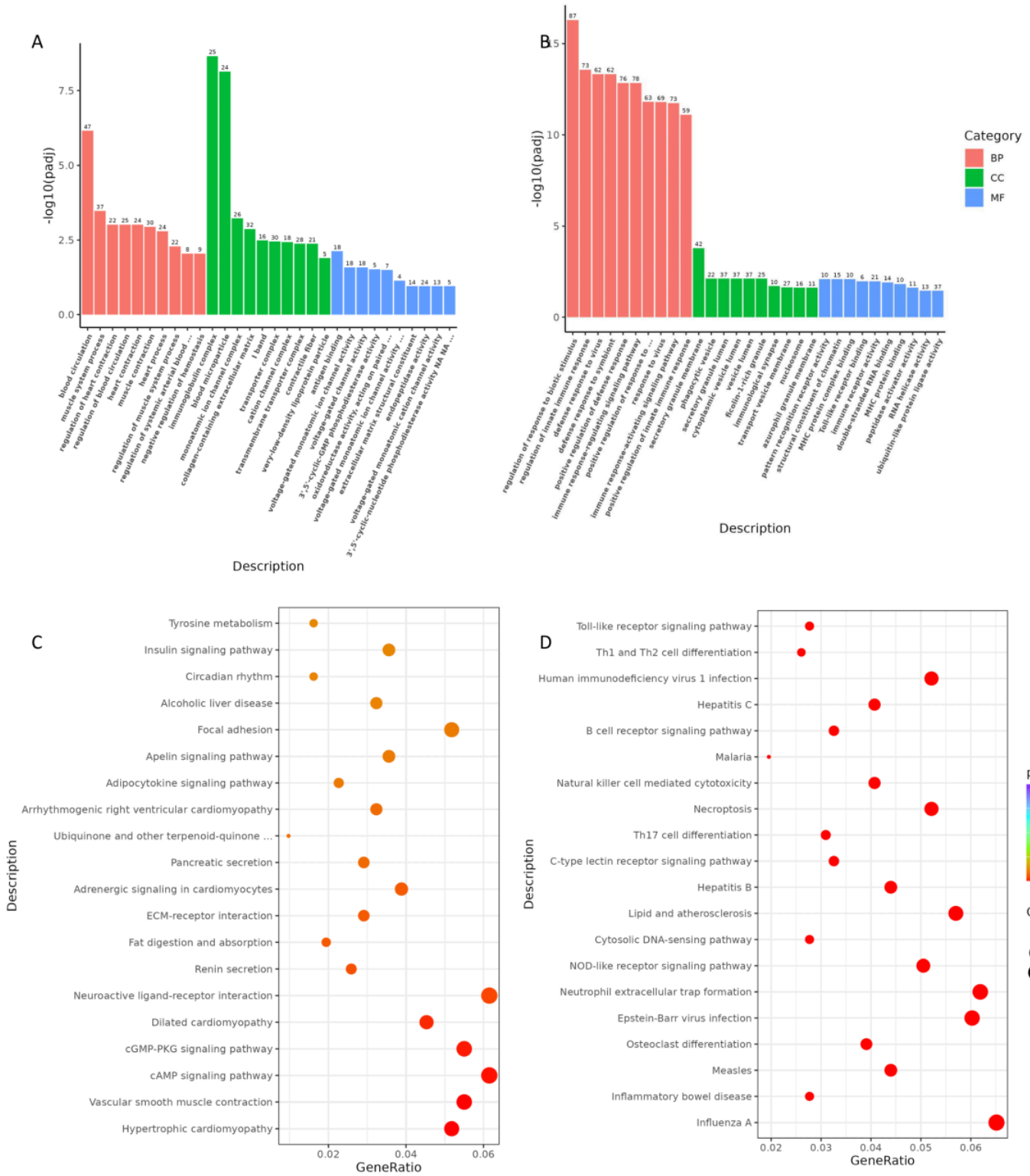


Figure 4

Gene Ontology (GO) analysis of upregulated (A) and downregulated (B) genes 24 h after hUC-MSCs injection; KEGG analysis of upregulated (C) and downregulated (D) genes 24h after hUC-MSCs injection.

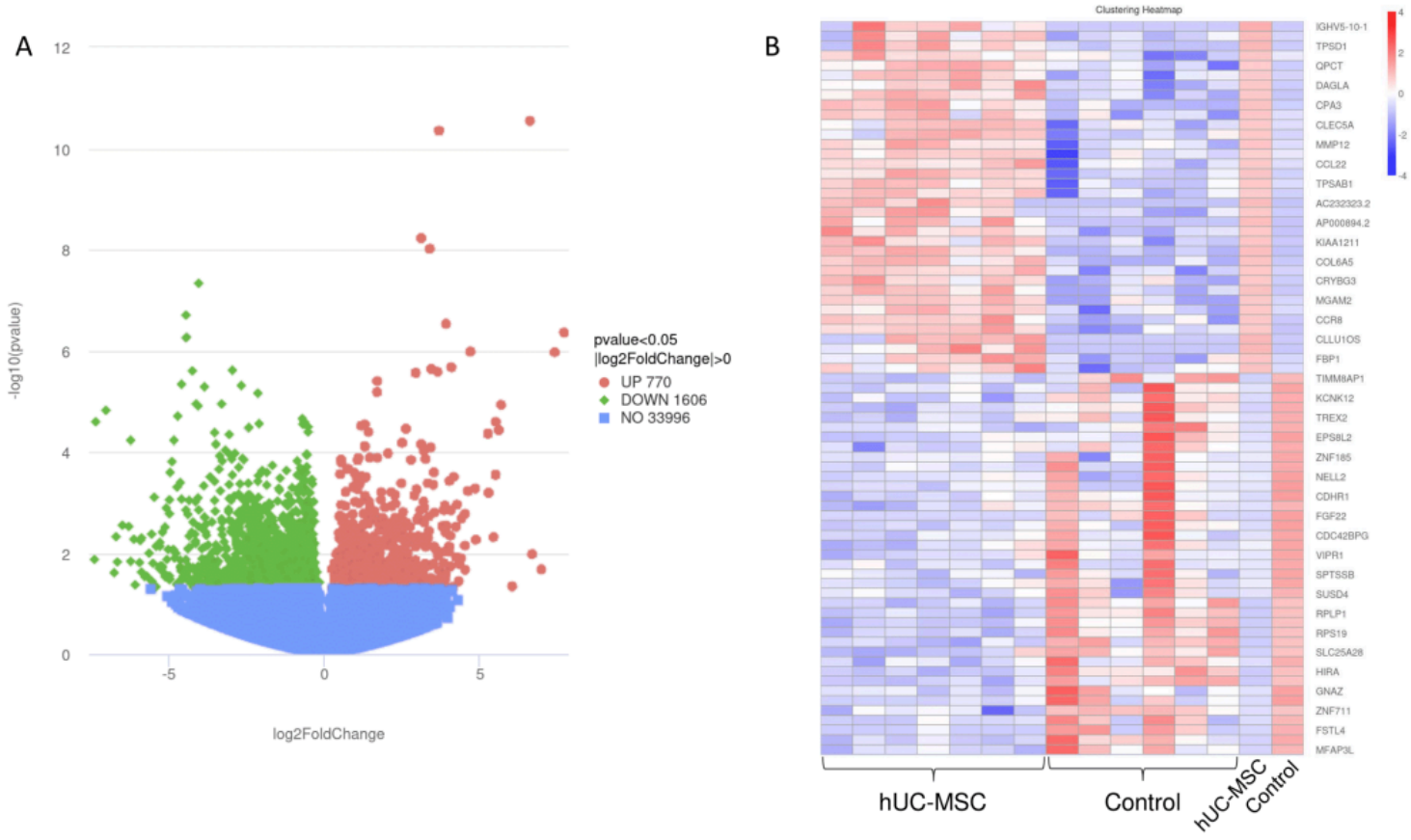


Figure 5

Differentially expressed genes (DEGs) in the MSC and control groups 7 days after hUC-MSCs injection. A) Volcano plot of DEGs; B) Heatmap of DEGs.

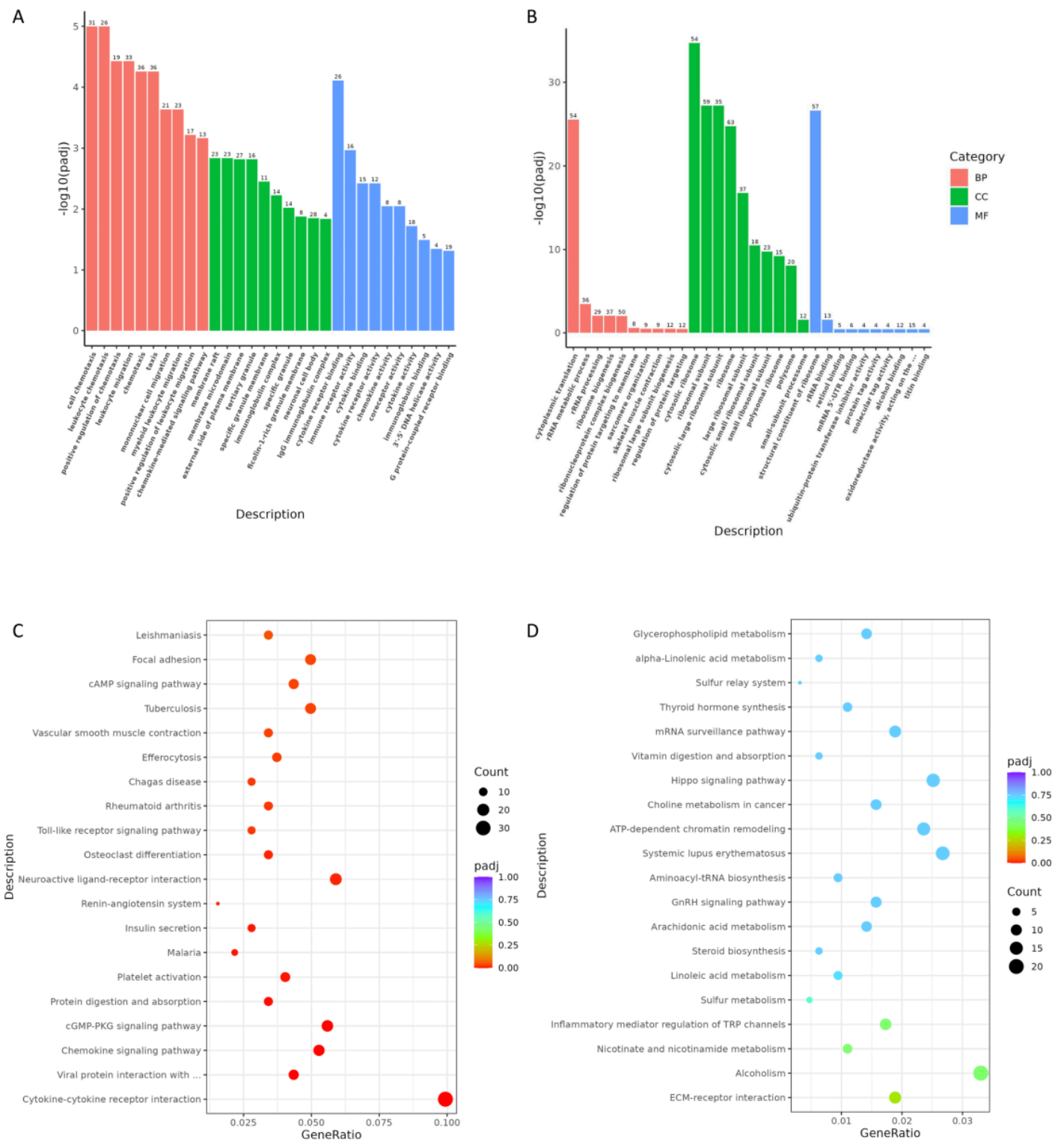


Figure 6

Gene Ontology (GO) analysis of upregulated (A) and downregulated (B) genes 7 days after hUC-MSCs injection; KEGG analysis of upregulated (C) and downregulated (D) genes 7 days after hUC-MSCs injection.

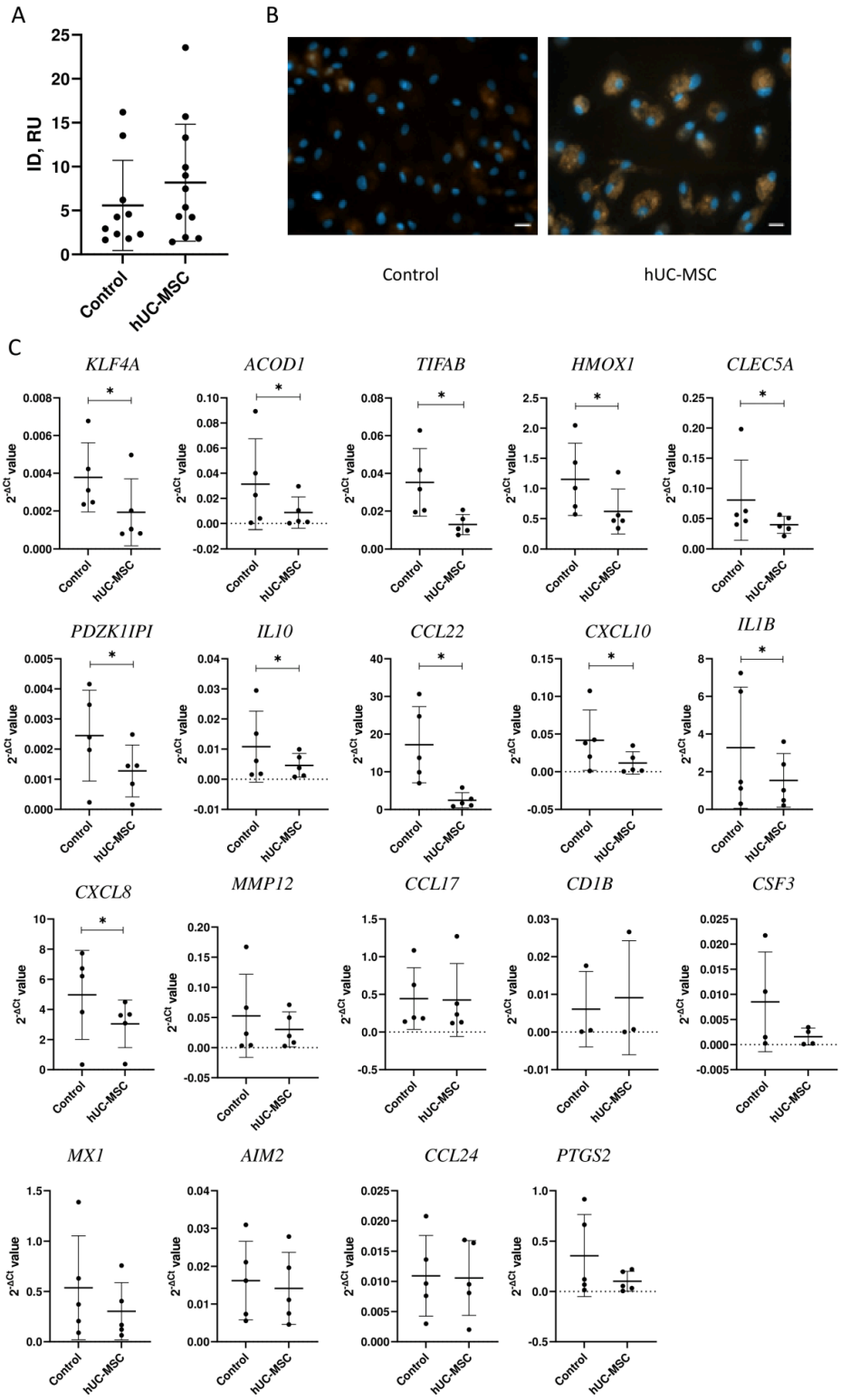


Figure 7

Effect of hUC-MSCs on macrophages *in vitro*. A) phagocytosis assay; B) representative micrographs of macrophages, scale bar 50 μm, Control – M1 pro-inflammatory macrophages without MSCs, red – measured signal from pHrodo™ Red BioParticles™ Conjugate at 585 nm, blue – nuclei stained with DAPI, 457 nm; C) RT-qPCR analysis. Data are presented as mean ± SD. Wilcoxon signed-rank test was used to compare the control and MSC groups: *, $p \leq 0.05$.

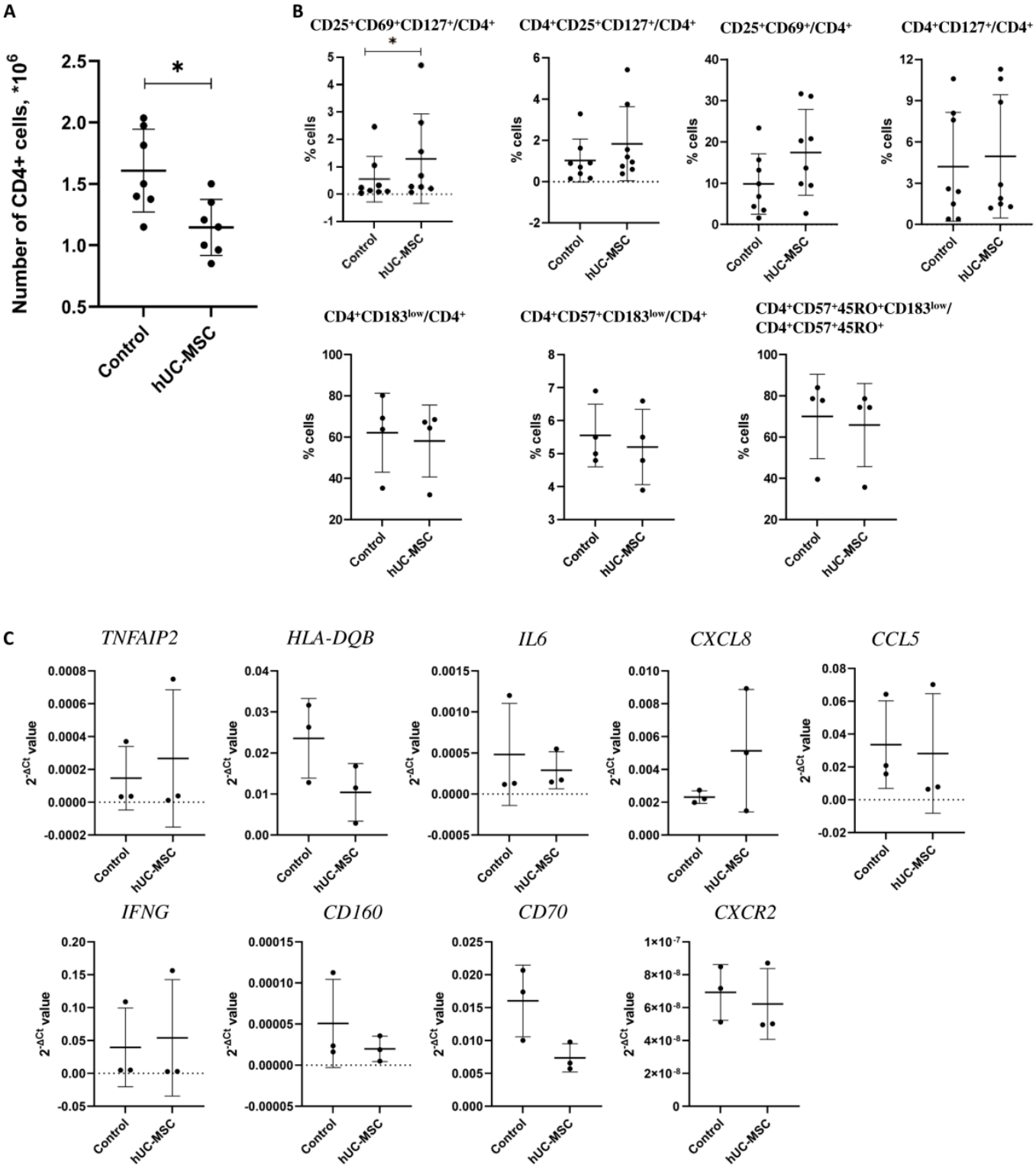


Figure 8

Effect of hUC-MSCs on CD4$^+$ cells *in vitro*. A) proliferation rate; B) immunophenotype analysis; C) RT-qPCR analysis. Data are presented as mean ± SD. Wilcoxon signed-rank test was used to compare the control and MSC groups: *, $p \leq 0.05$.

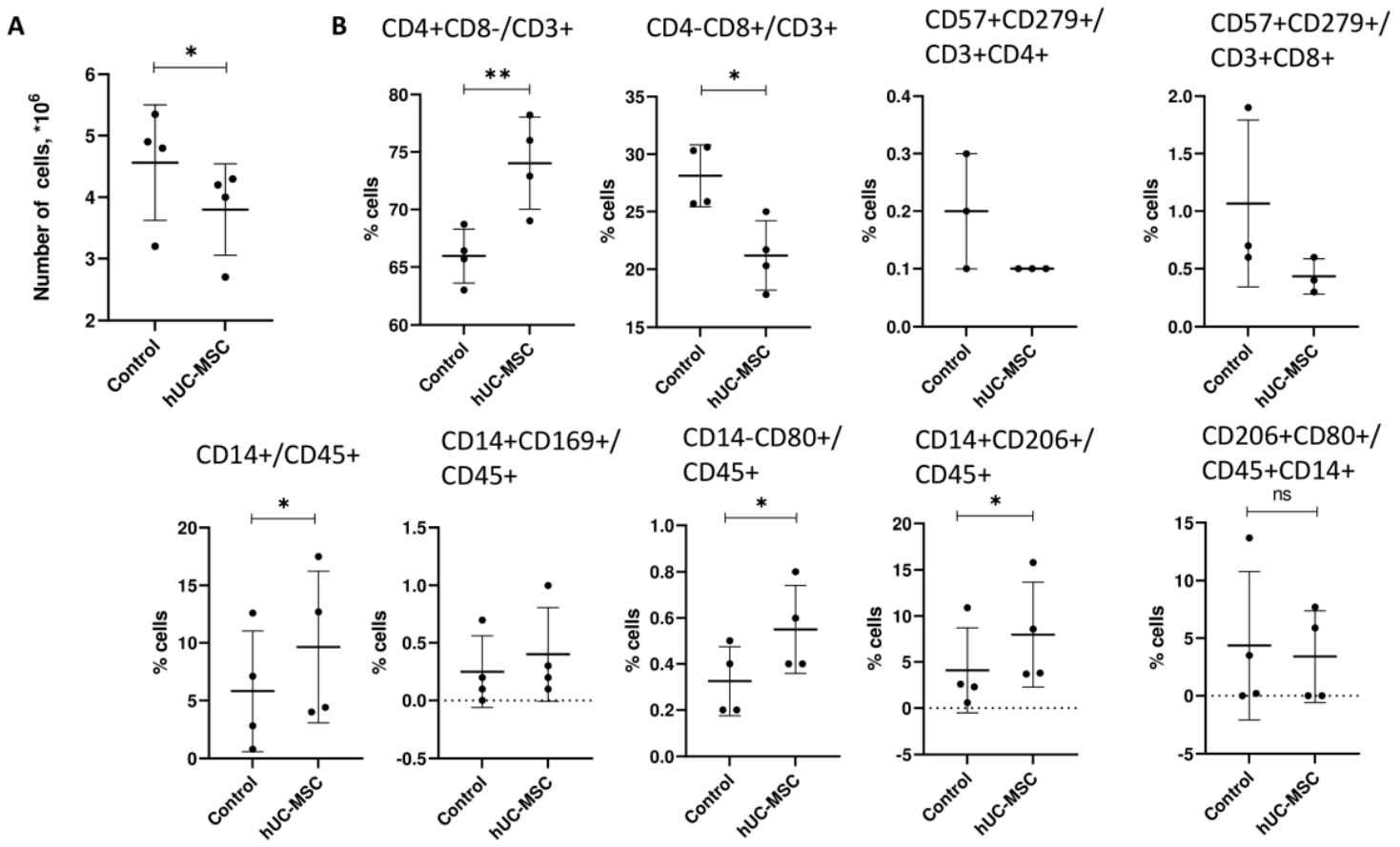


Figure 9

Effect of hUC-MSCs on PBMC *in vitro*. A) proliferation rate; B) immunophenotype analysis. Data are presented as mean ± SD. Wilcoxon signed-rank test was used to compare the control and MSC groups: *, $p \leq 0.05$; **, $p \leq 0.01$; ns, not significant.

Supplementary Files

This is a list of supplementary files associated with this preprint. Click to download.

- SupplementaryCharacterizationofhUCMSCs.pdf
- SupplementaryFigureS1.pdf
- SupplementaryFigureS2.pdf
- SupplementaryFigureS3.pdf
- SupplementaryFigureS4.pdf
- SupplementaryFigureS5.pdf
- SupplementaryFigureS6.pdf
- SupplementarytableS1.xlsx
- SupplementarytableS2.xlsx